ACS Catalysis

Research Article

pubs.acs.org/acscatalysis

Mechanistic Study of Alcohol Dehydration on γ-Al_2O_3

Sounak Roy,[†,∥] Giannis Mpourmpakis,[†,∥] Do-Young Hong,[‡,∥] Dionisios G. Vlachos,[†,∥] A. Bhan,[‡,∥] and R. J. Gorte*[,§,∥]

[†]Chemical and Biomolecular Engineering and [∥]Catalysis Center for Energy Innovation (CCEI), University of Delaware, Newark, Delaware 19716, United States

[‡]Department of Chemical Engineering and Materials Science, University of Minnesota, Minneapolis, Minnesota 55455, United States

[§]Department of Chemical & Biomolecular Engineering, University of Pennsylvania, Philadelphia, Pennsylvania 19104, United States

Supporting Information

ABSTRACT: The acid sites on γ-Al_2O_3 were characterized using FTIR spectroscopy of adsorbed pyridine and temperature programmed desorption (TPD) of 2-propanamine, ethanol, 1-propanol, 2-propanol, and 2-methyl-2-propanol, together with density functional theory (DFT) calculations. Following room-temperature adsorption and evacuation, the surface coverages of the adsorbed alcohols were between 2 and 3.2 × 10^{18} molecules/m^2. For each of the adsorbed alcohols, reaction to olefin and water products occurred in a narrow peak that indicated reaction is a first-order process with a well-defined activation energy, which in turn depended strongly on the particular alcohol. DFT calculations on an Al_8O_{12} cluster are in excellent agreement with the experimental observations and show that the transition states for dehydration had carbenium-ion character. The carbenium ion stability in terms of proton affinity (of alkenes) matches well with the activation energy of the dehydration reaction. Adsorption of water on the γ-Al_2O_3, followed by evacuation at 373 K, demonstrated that water simply blocks sites for the alcohols without affecting the reaction activation energy. There was no evidence for Brønsted sites on the γ-Al_2O_3 based on FTIR of pyridine or TPD of 2-propanamine.

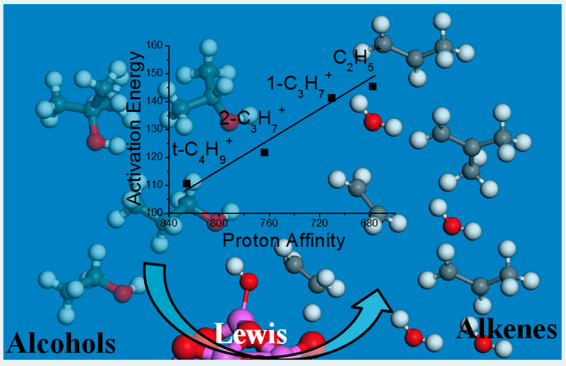

KEYWORDS: *alcohol dehydration, alumina, acid sites, reaction mechanism, TPD-TGA, DFT*

INTRODUCTION

While great progress has been made in understanding Brønsted acidity in solid acids like zeolites,[1] our understanding of Lewis acidity in solids like γ-Al_2O_3 is still incomplete. This is not because Lewis acidity in γ-Al_2O_3 is unimportant. For example, γ-Al_2O_3 has been used to carry out alcohol dehydration to olefins, where the presence of Brønsted sites can lead to undesired reactions, including skeletal isomerizations or double-bond shifts.[2] The Lewis acidity of γ-Al_2O_3 also precludes its use as a catalyst support in some applications, such as in hydrogenation of aldehydes, because of its high and undesired activity for aldol condensations.[3]

Numerous studies, both theoretical and experimental, have been carried out in an attempt to understand the nature of the Lewis sites in γ-Al_2O_3.[4−10] For example, Knözinger et al. proposed a reaction mechanism for the ethanol dehydration reaction, but the kinetic expressions derived from that mechanism did not fit the experimental data for the reaction.[4−6] Part of the complexity may be explained by findings from a recent paper by Kwak, et al.,[11] who reported that γ-Al_2O_3 has both Lewis sites (associated with Al^{3+}) and Brønsted sites (associated with OH groups formed by reaction of the penta-coordinate Al^{3+} with water), with the relative concentration of each of these changing with calcination temperature. These authors reported that both Lewis and Brønsted sites were active for dehydration of ethanol in temperature programmed desorption (TPD), although the Lewis sites gave reaction at slightly lower temperature, ∼25 degrees. Digne et al. performed density functional theory (DFT) calculations that indicated the stability of hydroxyl groups depends dramatically on the exposed facet, with sites on (100) facets undergoing dehydration by 600 K but sites on (110) remaining hydrated to temperatures hundreds of degrees higher.[8]

Clearly, our abilities to predict reaction chemistry and calculate kinetic barriers to reactions are still at an elementary stage; and questions remain even concerning the nature of the sites on γ-Al_2O_3. For example, the presence of Brønsted sites in γ-Al_2O_3 is usually inferred by the presence of surface hydroxyls. However, it has not been proven that hydroxyls on γ-Al_2O_3 are catalytically important or that they should be thought of as Brønsted sites. We are unaware of any evidence from classical experiments, such as identification of pyridinium ions in IR spectroscopy, which demonstrates these hydroxyls are able to protonate strong bases, let alone contribute protons to weaker

Received: March 16, 2012
Revised: June 26, 2012
Published: July 19, 2012

   dx.doi.org/10.1021/cs300176d | ACS Catal. 2012, 2, 1846−1853

bases like alcohols and olefins. Assuming that proton-transfer energetics on the solid γ-Al_2O_3 scales in one-for-one manner with gas-phase proton affinities, as has been found with Brønsted sites in zeolites,[12] the barrier for proton transfer from γ-Al_2O_3 to an alcohol would be very large. For example, if proton transfer from the alumina hydroxyls does not occur with pyridine, which has a proton affinity (PA) of 922 kJ/mol, the barrier for proton transfer would have to be much greater than 100 kJ/mol for alcohols like ethanol (PA = 796 kJ/mol) or simple olefins like ethylene (PA = 677 kJ/mol). We suggest the evidence that hydroxyl groups on γ-Al_2O_3 act as Brønsted sites remains unproven.

Shinohara et al. used semiempirical methods (PM3) to study the dehydration of alcohols on various oxides, including alumina.[13] Using silica as an example, they calculated the activation energies for decomposition of various adsorbed alkoxides for different mechanisms. Among the different mechanisms considered, one can identify E1 and E2 elimination mechanisms of the β-hydrogens of the alkoxides. In their calculations, the activation energies scaled with the carbenium-ion stability in an almost one-for-one manner if the rate-limiting step involved C−O bond scission of an adsorbed alkoxide. However, the activation energies for this mechanism were very high, >400 kJ/mol. For C−O bond scission with protonated oxygen, on the other hand, the calculated activation energies decreased to approximately 120 kJ/mol and were less dependent on the carbenium ion stability. Notice that this latter case should still be considered to be alcohol dehydration on Lewis-acid sites, since the protonated alkoxide forms the alcohol on an Al cation that is free from surface OH groups.

In this paper, we set out to examine whether hydroxyls on γ-Al_2O_3 could act as Brønsted sites and to use the concepts developed by Shinohara et al.[13] to better understand the dehydration of alcohols on this material. To simplify the reaction studies, we measured the relative reactivities of a series of alcohols, starting from the adsorbed state, using combined TPD-TGA (Thermogravimetric Analysis) in high vacuum. These results were then modeled using DFT methods. To look for Brønsted sites, we used FTIR of adsorbed pyridine and TPD-TGA of isopropylamine. Results from the combined experiments and calculations of alcohol dehydration on γ-Al_2O_3 suggest that the formation of adsorbed water is the driving force for the reaction under the conditions of our study. We did not find any evidence that γ-Al_2O_3 has Brønsted sites, even after exposure to water. Water simply blocks adsorption of the alcohol.

EXPERIMENTAL AND COMPUTATIONAL METHODS

Two γ-Al_2O_3 samples, one from Alfa Aesar and one from Fisher Scientific, were used as received and after treatment with aqueous, 1 M NH_4NO_3. For the NH_4NO_3 treatment, 500 mg of sample was stirred with 300 mL of the solution at 353 K for 3 h to reduce the Na contamination. The Na contents of the samples before and after treatment were quantified by flame atomic absorption spectroscopy (FAAS) using a Perkin-Elmer Analyst 400 Atomic Absorption/Emission Spectrometer and reported in Table 1. The surface areas of the samples are also shown in Table 1 and were determined from Brunauer−Emmett−Teller (BET) isotherms measured using N_2 at 78 K, after the samples had been degassed at 500 K. X-ray Diffraction pattern of the two Al_2O_3 samples are provided in the Supporting Information, Figure 1S. The profile matches well with the γ phase (JCPDS 48-0367), although a small amount of the χ phase (JCPDS 04-0880) was also observed.

Table 1. Surface Areas and Na Contents of Al_2O_3 Samples Used in This Study

catalysts	SSA (m^2/g)	Na content (ppm)	Na atoms per m^2 ($\times 10^{18}$)	percentage surface sites blocked[a]
fresh γ-Al_2O_3 (Alfa Aesar)	90	1319	0.383	20.15
NH_4^+ treated γ-Al_2O_3 (Alfa Aesar)	90	200	0.058	3.05
fresh γ-Al_2O_3 (Fisher Scientific)	150	1314	0.229	12.05
NH_4^+ treated γ-Al_2O_3 (Fisher Scientific)	150	302	0.053	2.79

[a]Assuming that the number of adsorption sites on γ-Al_2O_3 are 1.9×10^{18} per m^2.

TPD and TGA experiments were carried out simultaneously using a microbalance mounted within a high vacuum chamber. The base pressure of the system was 1×10^{-8} Torr. The sample weight was continuously monitored using a CAHN 1000 microbalance, and the desorbing species were monitored using a UTI quadrupole mass spectrometer. The sample temperature was measured with a thermocouple placed near the sample, and the heating rate during desorption was maintained at 10 K/min by a temperature controller. Unless otherwise stated, the samples were heated in vacuum to 773 K and then cooled in vacuum, prior to exposure to the alcohols. Each of the different alcohols was adsorbed at room temperature by exposing the sample to 3 Torr of vapor until there was no further uptake, as determined by weight changes using the microbalance. The system was then evacuated for 1 h before beginning the TPD-TGA experiment. The only species leaving the sample were the unreacted alcohol and its olefin and water products. No ether formation was observed under the conditions of this study. In all cases, the weight of the Al_2O_3 samples returned to their original values after an adsorption−desorption cycle.

Because it has been suggested that Brønsted sites may exist on γ-Al_2O_3 after some pretreatment conditions, the nature of the acid sites on our samples was examined using two different methods. In the first method, TPD-TGA measurements were performed following adsorption of 2-propanamine. It has previously been shown that 2-propylammonium ions decompose to form NH_3 and propene between 575 and 650 K, so that any Brønsted site strong enough to protonate the amine would be observed by the reaction.[1] The second method, infrared spectroscopy with adsorbed pyridine, was used to look for pyridinium ions. With the pyridine IR measurements, the γ-Al_2O_3 was pretreated in water vapor at various temperatures in an attempt to produce hydroxyls that might have Brønsted-acid character. Infrared spectra were measured with 2 cm^{-1} resolution on self-supporting wafers (3 cm^2, 20−40 mg) held within a quartz vacuum cell with NaCl windows using a Nicolet 6700 IR spectrometer equipped with a mercury cadmium telluride (MCT) cryodetector. The sample was treated to 773 K in flowing dry air (0.0167 K s^{-1}) and degassed at this temperature for 1 h (4.0×10^{-2} Torr) prior to contact with pyridine vapor (2 Torr) at ambient temperatures. The sample was exposed to pyridine vapors for 0.5 h at that pressure prior to degassing for 1 h to remove physisorbed pyridine. In a separate experiment, after pretreatment and degassing at 773 K, the sample was cooled to 573 K prior to introducing water (8

dx.doi.org/10.1021/cs300176d | ACS Catal. 2012, 2, 1846−1853

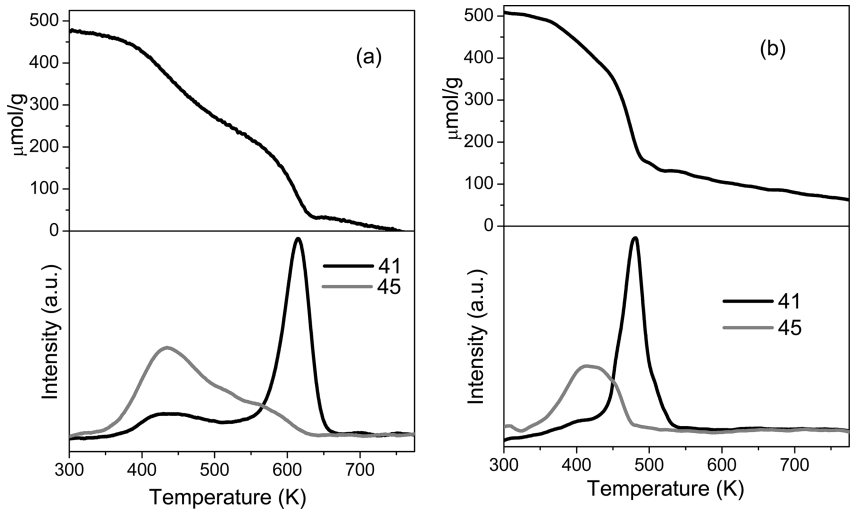

Figure 1. TPD-TGA curves for 2-propanol over (a) as received fresh γ-Al_2O_3 (from Alfa Aesar) and (b) NH_4^+ ion exchanged γ-Al_2O_3 (from Alfa Aesar).

Torr) for 20 min; and, subsequently, the sample was cooled to ambient temperatures under vacuum and exposed to pyridine (2 Torr) for 0.5 h, then degassed for 1 h prior to recording IR spectra.

The dehydration mechanism for primary (ethanol, 1-propanol), secondary (2-propanol), and tertiary (2-methyl-2-propanol) alcohols was also investigated on a Lewis acid site of an Al_8O_{12} cluster by means of DFT calculations. We used the Becke's three-parameter hybrid (B3LYP) functional[14,15] with the 6-311G* triple-ζ basis set as implemented in Gaussian 09.[16] All reaction pathways were first mapped by scanning the potential energy surface of the reaction coordinate. The energy maximum that was found along the reaction coordinate was fully relaxed to a saddle point to locate the actual transition state (TS). All TSs and local minima were obtained by full optimizations and verified by vibrational frequency and Intrinsic Reaction Coordinate (IRC) calculations.

RESULTS AND DISCUSSION

TPD-TGA Results for Alcohols. Previous TPD studies of 2-propanol on various aluminas showed that Na has a very strong effect on the temperature at which reaction occurs.[17] Therefore, we started our investigation with TPD-TGA experiments with 2-propanol on the two γ-Al_2O_3 samples, before and after pretreatment to remove Na. Table 1 shows the NH_4NO_3 treatment significantly reduced the Na content of both samples without changing the surface areas. However, this treatment had a dramatic effect on the TPD-TGA results, as indicated by the results in Figure 1.

Figure 1a was obtained following adsorption of 2-propanol on the untreated Alfa Aesar sample. On the basis of the weight change after adsorption and evacuation at room temperature, approximately 480 μmol/g of the alcohol remained on the surface, corresponding to a specific surface coverage of 3.2×10^{18} molecules/m^2. The TPD results indicate that desorption occurred in two temperature regions, with unreacted alcohol (m/e = 41 and 45) leaving the sample below 550 K and propene (m/e =41) desorbing in a peak centered at ~610 K. Because water desorbed over a broad range of temperatures, no peak was observed, although all of the water did leave the sample because the sample weight returned to its initial value. The TGA results indicate that approximately 200 μmol/g of the alcohol reacted to the olefin and water products. Figure 1b was obtained from the same sample after it had been treated to remove Na. The coverage of 2-propanol after adsorption and evacuation at room temperature was nearly the same as on the untreated sample, 500 μmol/g. The amount of 2-propanol that desorbed as propene and water was also approximately the same, 200 μmol/g; however, the peak temperature for propene reaction decreased from 610 K to ~490 K.

Figure 2 shows TPD-TGA data for 2-propanol on the NH_4NO_3-treated, Fisher Scientific sample. The initial coverage

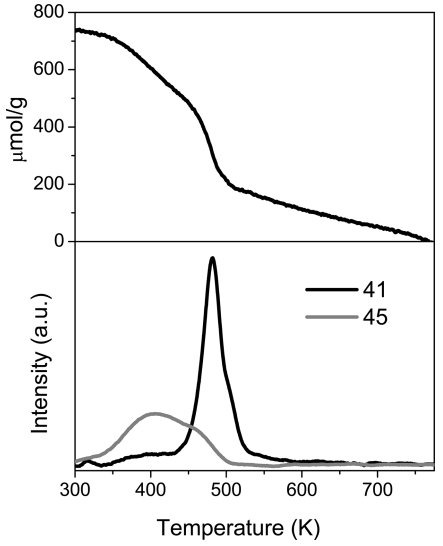

Figure 2. TPD-TGA curves for 2-Propanol over NH_4^+ ion exchanged γ-Al_2O_3 from Fisher Scientific, (SSA = 150 m^2/g).

of 2-propanol after evacuation was 740 μmol/g. On a surface area basis, this is 3.0×10^{18} molecules/m^2, a specific coverage very close to that observed with the Alfa Aesar alumina. The amount of alcohol that left the sample as propene and water was ~400 μmol/g, a number that corresponds to a slightly higher fraction of the total adsorbed alcohol than was found with the Alfa Aesar sample. However, the formation of propene occurs at exactly the same temperature, 490 K.

dx.doi.org/10.1021/cs300176d | ACS Catal. 2012, 2, 1846–1853

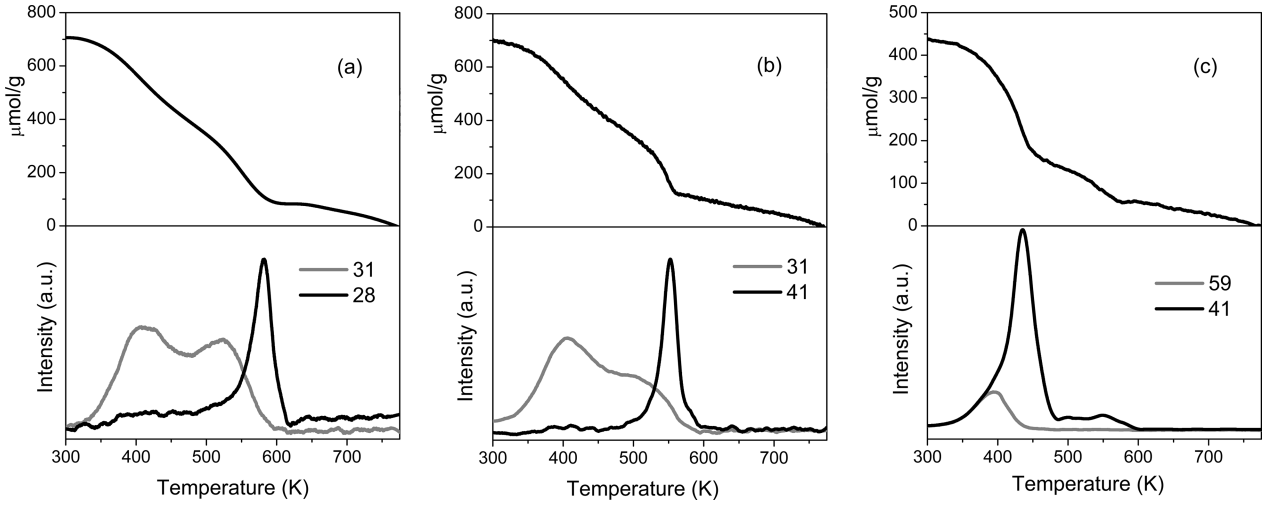

Figure 3. TPD-TGA results for (a) Ethanol, (b) 1-Propanol, and (c) 2-methyl-2-Propanol over NH_4^+ ion exchanged Al_2O_3 (from Fisher Scientific).

The results in Figures 1b and 2 lead to several important conclusions. First, two very different γ-Al_2O_3 samples gave nearly identical results for 2-propanol desorption after they had been treated with NH_4NO_3. This suggests that treated γ-Al_2O_3 has an intrinsic reactivity that can be reproduced and characterized. Second, the propene product peaks in TPD are narrow and well-defined, suggesting that the reaction sites are similar in their ability to catalyze the dehydration reaction. Because propene is only very weakly adsorbed on γ-Al_2O_3, the desorption temperature for propene can be used to deduce an activation energy for the dehydration reaction of the adsorbed alcohol. If one assumes first-order kinetics and a normal reaction pre-exponential of 10^{13}/s, application of the Redhead Equation leads to an activation energy of 141 kJ/mol.[18] It is important to recognize that this activation energy corresponds to the reaction of the adsorbed 2-propanol and should not be applied to steady-state reaction conditions, where the surface conditions of the catalyst could be very different and where surface reaction rates would be coupled with adsorption and other surface processes.

We also obtained TPD-TGA results following the adsorption of two primary alcohols, ethanol and 1-propanol, and a tertiary alcohol, 2-methyl-2-propanol, on the Fisher γ-Al_2O_3, with results shown in Figure 3. The data are qualitatively similar to those obtained for 2-propanol. For ethanol and 1-propanol, the surface coverage following adsorption and 1 h evacuation at room temperature was ~700 μmol/g, with approximately 200 μmol/g undergoing reaction to olefin and water products. The similarity in coverages indicated that each of the alcohols is probing the same sites. With 2-methyl-2-propanol, the initial alcohol coverage was lower, 450 μmol/g, because of the bulkier nature of this molecule; and the amount that reacts, ~400 μmol/g, appears to be somewhat higher. Desorption of unreacted ethanol (m/e = 28 in Figure 3a) and 1-propanol (m/e = 31 in Figure 3b) occurs in two regions, with broad peaks near 400 and 500 K. Because interpretation of TPD curves from porous samples is complex for molecules that can readsorb, it is probably not trivial how to interpret the multiple desorption features.[19]

A result that is clear from the data in Figure 3 is that the olefin products form over a very narrow temperature range for each of the adsorbed alcohols, and the peak temperatures at which the products form depend strongly on the type of alcohol. Whereas the formation of propene from adsorbed 2-propanol occurred at 490 K, the olefin products from ethanol, 1-propanol, and 2-methyl-2-propanol formed at 580, 550, and 435 K, respectively. The fact that the peak reaction temperature increased when moving from the tertiary, to the secondary, to the primary alcohols implies that the TSs for the reaction must have some carbenium-ion character, since the strength of the C−OH bonds does not vary significantly with the different alcohols (See Table 3, vide infra). Again assuming a normal pre-exponential of 10^{13}/s for the reaction and applying the Redhead Equation, the activation energies for the dehydration of each of the alcohols were determined. These are reported in Table 2.

Table 2. Experimental Activation Energies

alcohol	E_a (kJ/mol)
ethanol	145
1-propanol	141
2-propanol	121
2-methyl-2-propanol	110

In all of the experiments described above, the γ-Al_2O_3 samples were first heated to 773 K in vacuum, conditions that are expected to produce Lewis-Acid sites. In the classical picture, adsorption of water onto these Lewis sites should produce Brønsted-acid sites that could have very different reactivity. To look for this, we exposed the NH_4NO_3-treated, γ-Al_2O_3 from Fisher Scientific to 3 Torr water vapor at 373 K. The sample was then evacuated at 373 K and cooled to room temperature, before exposing it to 2-propanol. The amount of water remaining on the sample after evacuation at 373 K was approximately 0.0336 g H_2O/g alumina, or 1800 μmol/g. Exposure to 2-propanol was performed as before.

The TPD-TGA results obtained in this case are shown in Figure 4, with the TGA results reported using the molecular weight of 2-propanol and the zero corresponding to the weight of the γ-Al_2O_3 immediately before exposure to 2-propanol. Negative weights here correspond to desorption of water. The main effect of water adsorption was to reduce the amount of 2-propanol that adsorbs from 740 μmol/g to less than 200 μmol/g, with the fraction that reacts decreasing proportionally. There was no change in the temperature at which 2-propanol reacts or

dx.doi.org/10.1021/cs300176d | ACS Catal. 2012, 2, 1846−1853

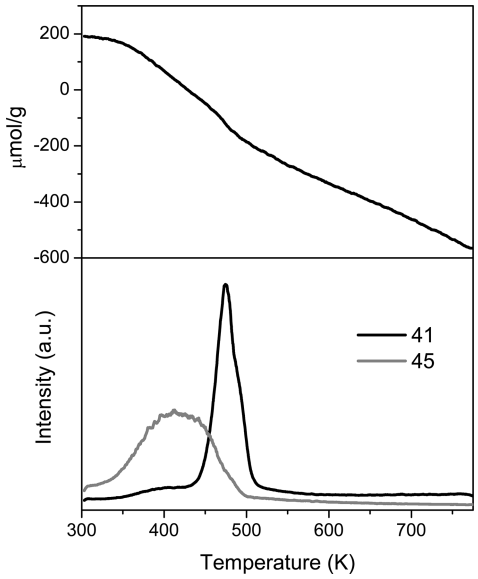

Figure 4. TPD-TGA results for 2-Propanol over water preadsorbed NH_4^+ ion exchanged γ-Al_2O_3. Water was adsorbed around 100 °C followed by 2-Propanol adsorption in UHV at room temperature.

in the fraction of 2-propanol that reacts, as measured by the relative areas under the m/e = 41 and 45 peaks. The main conclusion from Figure 4 is that water simply blocks adsorption of the alcohol. Furthermore, most of the water was not displaced by the alcohol, even though the alcohol was present in large excess by having been exposed subsequent to evacuation of water at 373 K, suggesting that water is bound more strongly than is the alcohol. Finally, there is no evidence for the formation of new sites due to the presence of water. The relatively small amount of 2-propanol that does adsorb is likely due to displacement of some water by the alcohol during the adsorption process.

Computational Results for Alcohol Dehydration. Ab-initio calculations were performed to gain mechanistic insights into the alcohol dehydration reaction on Lewis acid sites of alumina. We studied first the C−OH bond dissociation behavior (OH group removal) of the different alcohols (ethanol, 1-propanol, 2-propanol, 2-methyl-2-propanol) in the gas-phase. Detailed potential energy scans of the C−OH bond distance elongation under different spin states can be found in the Supporting Information, Figure 2S. In Table 3 we present the C−OH dissociation enthalpies of the alcohols, and we include for comparison purposes the C−H dissociation enthalpies of the corresponding alkanes. The C−OH dissociation appears to be independent of the type of the alcohol (vide supra), whereas the C−H dissociation depends on the substitution degree of an alkane. Specifically, the C−OH bond dissociation enthalpy difference between the various alcohols is 4.7 kJ/mol, whereas it becomes 30.5 kJ/mol for the C−H bond of the alkanes.

Table 3. C-X Bond Dissociation Enthalpies of $C_nH_{2n+1}X$ organic complexes when X = H (alkanes) and X = OH (alcohols)[a]

type of organic complex	X = H (gas phase)[b]	X = OH (gas phase)	X = OH (on Al_8O_{12})
C_2H_5-X	413.0	372.4	323.2
n-C_3H_7-X	415.5	374.4	325.6
i-C_3H_7-X	397.1	373.0	327.4
t-C_4H_9-X	385.0	369.7	327.7
max bond dissociation enthalpy difference	30.5	4.7	4.5

[a]Values are in kJ/mol. [b]Our DFT calculated C−H bond dissociation enthalpies of the alkanes are in very good agreement with tabulated experimental values presented in ref 29.

The next step was to investigate the actual dehydration reaction on alumina. We constructed a highly symmetric, Al_8O_{12} model cluster, which originated from bulk aluminum oxide. This cluster shows S6 point group symmetry, maintains the stoichiometry of the bulk (see Figure 5a) and is very robust

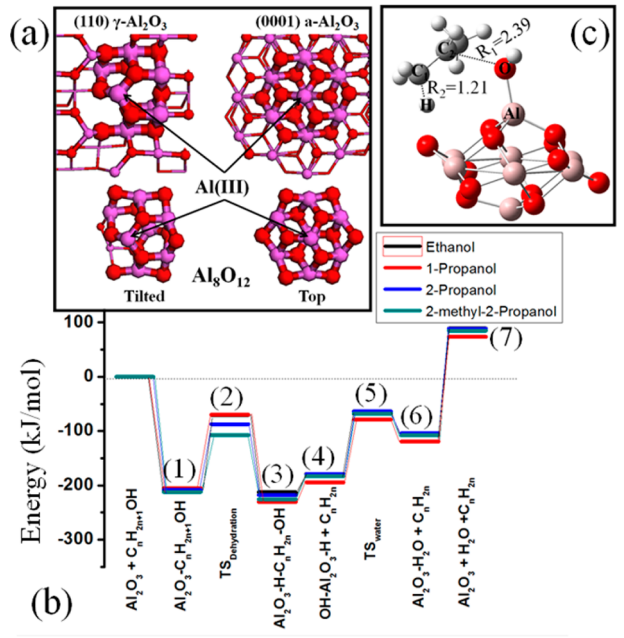

Figure 5. (a) Construction of the Al_8O_{12} model-cluster representing tricoordinated Al sites on dehydrated (110) γ-Al_2O_3 and (0001) α-Al_2O_3. (b) DFT calculated Lewis-catalyzed alcohol dehydration mechanism on the Al_8O_{12} model-cluster. The steps are as follows: (1) adsorption, (2) dehydration TS, (3) Alkene formation, (4) Alkene desorption, (5) water formation TS, (6) water formation, and (7) water desorption. (c) Structural characteristics of the TS (step 2 in panel b) in the concerted dehydration mechanism of 2-propanol (OH group on Al and β-hydrogen on surface O).

against relaxations. The central Al atom of the cluster is tricoordinated, evolving from the T_d sites of the bulk, with one oxygen atom removed. The peripheral Al atoms are tetra-coordinated. The oxygen atoms, neighboring to the central Al, are tricoordinated. Tricoordinated oxygens are typically found in both (110) and (100), the common catalytic phases of γ-Al_2O_3. The selection of tricoordinated Al site over a tetra-coordinated (both present on the (110) surface of γ- Al_2O_3) or a penta-coordinated Al site (present on the (100) surface) was based on Lewis acidity. Tricoordinated Al sites are expected to be stronger Lewis acids compared to Al with other coordinations.[20] As shown in Figure 5 a, this cluster structurally represents the local chemical environment of tricoordinated Lewis sites on both the (0001) α-Al_2O_3[21] and (110) γ-Al_2O_3 (see highlighted atoms). The tricoordinated Al sites of the fully dehydrated (110) termination of γ-Al_2O_3 (also referred to as "defect sites") are reported to be strong, Lewis type of catalytic acid sites.[22,23] The Al_8O_{12} cluster (see tilted view in Figure 5 a)

dx.doi.org/10.1021/cs300176d | ACS Catal. 2012, 2, 1846−1853

consists of an Al_7O_{11} part of the (110) γ-Al_2O_3 (highlighted atoms) having additionally one Al and O atom (atoms in stick representation). These atoms saturate the peripheral dangling bonds, maintain the stoichiometry of the bulk, and finally stabilize the cluster. Previous detailed ab initio calculations[21] have shown that the Al_8O_{12} cluster can accurately reproduce periodic DFT and experimental values of surface relaxation parameters and energies of α-Al_2O_3 surface. Thus we believe that our cluster adequately captures the surface chemistry.

We investigated various dehydration mechanisms, including an alkoxy intermediate through an E1 type mechanism, as recently proposed.[24] However, we found that the E1 mechanism through alkoxy formation proceeds with high barriers, as shown in the Supporting Information, Figure 3S. An energetically more favorable pathway is a concerted dehydration mechanism, where the surface Al acid-site extracts the OH group and a surface O base-site the β-hydrogen of the alcohols. We characterize this mechanism as a concerted E2 type of reaction. The energy diagram of this concerted mechanism is presented in Figure 5b, and the detailed mechanistic scheme and associated structures in the Supporting Information, Figure 4S. The first step of the mechanism is alcohol adsorption on the Al-Lewis site. The alcohol strongly interacts with the Al site through the O of the hydroxyl group, in agreement with periodic slab calculations.[10,25] In the next step, H is transferred from the secondary C of the alcohol to a surface O atom of the alumina (We investigated transfer to both two- and tricoordinated O atoms; see Supporting Information, Figure 3S.). This results in the formation of the alkene, which easily desorbs to the gas-phase. To complete the catalytic cycle, water is formed on the surface from the remaining H and OH groups from the alcohol dehydration reaction. Finally, water desorbs into the gas-phase and the catalyst is regenerated. The dehydration barriers (TS1 in Figure 5) for the different alcohols with respect to their adsorbed state were calculated to be as follows: ethanol = 134.7, 1-propanol = 135.6 kJ/mol, 2-propanol = 120.9 kJ/mol, and 2-methyl-2-propanol = 104.6 kJ/mol. These values are in very good agreement with the experimental activation energies for ethanol, 1-propanol, 2-propanol, and 2-methyl-2-propanol (see Table 2).

In Figure 5c, we present the TS for 2-propanol dehydration. In the TS, the C−OH bond of the alcohols (R_1) is elongated significantly. For instance, the R_1 distance of 2-propanol is 1.43 Å in the gas-phase, 1.50 Å in the adsorbed state, and 2.39 Å in the TS. On the other hand, the β-hydrogen bond with the C_2 carbon (R_2) is less elongated in this concerted mechanism compared to the R_1 (R_2 is 1.09 Å in both gas-phase and adsorbed case and 1.21 Å in the TS). As a result, the TS is late and can be considered as an alcohol with a separated OH group and a slightly perturbed β-hydrogen, that is, as a carbocation stabilized by the presence of a OH group. This R_2 elongation gives to the TS carbenium-ion characteristics. Natural bond orbital (NBO) charge analysis revealed that there is a charge separation at the TS. The C_3H_7 species of 2-propanol is charged +0.71|e$^-$| on the TS and +0.45|e$^-$| and +0.30|e$^-$| in the adsorbed and gas-phase states, respectively. On the other hand, the OH group of the alcohol is charged −0.61|e$^-$|at the TS and −0.31|e$^-$| and −0.30|e$^-$| in the adsorbed and gas-phase, respectively. A detailed structural and NBO charge analysis for all the alcohols is presented in the Supporting Information, Table 1S.

It should be noted that our computed alcohol dehydration TS has similar structural characteristics with a propane dehydrogenation TS of a concerted mechanism on the tricoordinated Al sites of (110) γ-Al_2O_3, using periodic DFT.[25] Moreover, the barrier of propane dehydrogenation was reported to be 127 kJ/mol, close to our calculated barrier of 120.9 kJ/mol for the corresponding 2-propanol dehydration, on the same Lewis sites of γ-Al_2O_3. A similar dehydration mechanism through an E2 elimination reaction of the β-hydrogen of 2-butanol over γ-Al_2O_3 (100) surface and nanochannels has been proposed by Dabbagh et al.[26] Their calculated dehydration barriers were larger than the ones we report. This is probably due to the penta-coordination of the Al Lewis-sites present on the (100) planes of γ-Al_2O_3. Finally, in agreement with the results presented in Supporting Information, Figure 3S (on tricoordinated Al sites), preliminary periodic DFT calculations on penta-coordinated Al sites on γ-Al_2O_3 suggest that the concerted E2 dehydration reaction mechanism is more favorable than an E1 mechanism through the alkoxy formation (results not shown here).

Since both the experimental and the theoretical results showed that the activation energies decreased in going from primary, to secondary, to tertiary alcohols, we sought a descriptor which could relate the activation energies to a property of the alcohols, specifically, the stability of the carbenium ion that would be formed by removal of OH. The reason is 2-fold: First, the TS for the dehydration of the alcohols has carbenium-ion character, as we pointed out above; and, second, the Carbenium Ion Stability (CIS) follows the trend primary < secondary < tertiary. The CIS can be quantified from gas-phase calculations as the PA of the alkenes to form the carbenium ion. In other words, it is the energy (absolute value) of the reaction $C_nH_{2n} + H^+ \rightarrow C_nH_{2n+1}^+$ (CIS = PA(alkenes)) = $|E_{\text{carbenium ion}} - E_{\text{alkene}}|$, where $E_{\text{carbenium ion}}$ and E_{alkene} are the total electronic energies of the $C_nH_{2n+1}^+$ and C_nH_{2n} species, respectively. We found that the activation energies can be correlated with the CIS via a linear relationship, as shown in Figure 6 (activation energies for dehydration on both two- and tricoordinated surface O). It is worth noting that the slope of the linear relationship is approximately 0.25. The reason we did not observe a one-for-one manner between the activation energies and the carbenium-ion stability of the various alcohols is because the dehydration mechanism evolves

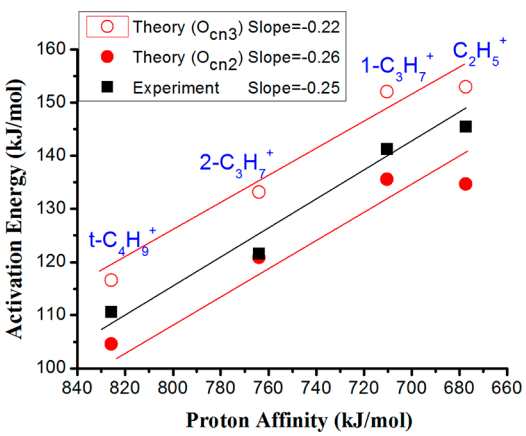

Figure 6. Activation energy vs PA (squares: experimental results; circles: theoretical results involving dehydration on a two- coordinated (closed symbols) and three-coordinated (open symbols) O atom.

dx.doi.org/10.1021/cs300176d | ACS Catal. 2012, 2, 1846−1853

through a TS with carbenium-like characteristics, without actually stabilizing any carbenium-ion as intermediate during the reaction. This mechanism is significantly different from the dehydration of alcohols on Brønsted sites of solid acids where a carbenium-ion is stabilized as an alkoxide on the pores of a zeolite.[1]

The concerted E2-type, dehydration mechanism we propose involves both (Lewis) acid and base centers on the alumina surface. The surface-Al acid centers are responsible for extracting the OH group, whereas, the surface-O base centers the β-hydrogen of the alcohols. As a result, the acid and base strength of the Al and O sites, respectively, determines the dehydration barriers on different catalytic sites. However, the slope of ~0.25 for the dehydration of different alcohols (Figure 6) is not expected to change dramatically when the same mechanism happens on acid and/or base centers of different strength. This is illustrated by the nearly parallel lines connecting the open and closed circles that correspond to different base centers (two- and tricoordinated surface O). This is because the descriptor of this linear relationship is an intrinsic property of the alcohols, that is, the CIS. It should be noted from Figure 6 that the basicity of the O atoms is less important than the CIS of the alcohols. The alcohol dehydration barriers change by ~15 kJ/mol on the different coordinated O atoms and by ~33 kJ/mol depending on the alcohol type (CIS). As a final step to ensure that the relationship between the dehydration barriers of the alcohols and the CIS holds because of the TS characteristics and not because of the C−OH bond dissociation behavior between the different alcohols, we calculated the C−OH bond dissociation of the different alcohols on the Al_8O_{12} cluster. These results are included in Table 3 with the aforementioned gas-phase calculations, verifying once again that the C−OH bond dissociation (even on alumina) is independent of the type of the alcohol.

In addition to the dehydration mechanism, Figure 5 reveals an important feature concerning water adsorption. The barrier for water desorption is significant (TS water formation = 115.4 kJ/mol in Supporting Information, Figure 4S). In fact, the total desorption energy was calculated to be 193.0 kJ/mol, in very good agreement with the experimental value for the heat of adsorption, −190 kJ/mol.[27] The water desorption value is larger than the activation energies of the alkenes formation, explaining how water can poison the surface, as seen in Figure 4.

Finally, our cluster model, being a local-reactivity model, may not be able to capture quantitatively the doping effects from the presence of Na^+ (sodium content on the surface) because of the curvature and nanometer size of the cluster. With this in mind, we have performed DFT calculations on Na^+ doped Al_8O_{12} cluster that provided a possible explanation on the effect of sodium, namely, as follows. (i) Na^+ preferentially interacts with strong basic centers of the cluster, which are the two-coordinated O sites (O_{cn2}). As a result, the basicity of these centers decreases. Figure 6 indicates that alcohol dehydration involving weak basic-centers (O_{cn3}) on alumina surface proceeds with higher barriers than when involving strong basic-centers (O_{cn2}). (ii) The presence of sodium cations can affect the dehydration barriers on neighboring surface basic centers. The ethanol dehydration barrier involving tricoordinated O (O_{cn3}) of Al_8O_{12} is 153.0 kJ/mol, which increases to 166.2 kJ/mol when the peripheral two-coordinated O sites of the cluster (O_{cn2}) are doped with Na^+ (see the Supporting Information, Figure 5S). As a result, we expect that the presence of sodium on the surface of γ-Al_2O_3 will increase the dehydration barriers of the alcohols.

Determination of Brønsted or Lewis Acidity. To determine whether the acid sites on the γ-Al_2O_3 had Brønsted or Lewis character, we first performed TPD-TGA measurements of 2-propanamine on the Alfa Aesar sample after it had been heated in vacuum 773 K (Figure 7). Exposure to 3 Torr of

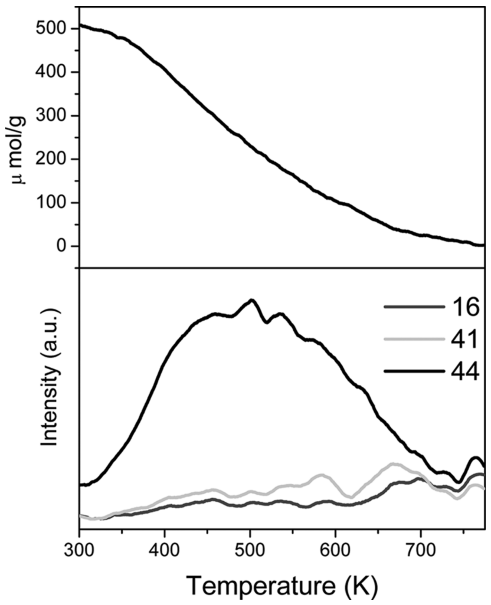

Figure 7. TPD-TGA profiles for isopropylamine over NH_4^+ ion exchanged Al_2O_3 sample.

2-propanamine, followed by evacuation, left 500 μmol/g of the amine on the surface. All of the amine desorbed intact over a broad temperature range, from 350 to 700 K, with no evidence for the formation of ammonia and propene between 575 and 650 K, as would have been observed if there were Brønsted sites strong enough to protonate the amine.[1]

We also examined the sample using infrared spectroscopy of adsorbed pyridine, with the results shown in Figure 8. Figures 8a and 8b show room-temperature spectra in the region from 1300 to 1800 cm^{-1} for the γ-Al_2O_3 sample after evacuation for 1 h at 773 K and after exposure to 8 Torr of water vapor at 573 K for 20 min, followed by evacuation at 573 K. With the lower dehydration temperature, an additional broad band, centered at 1640 cm^{-1}, is also observed in the spectrum of Figure 8b, and this can be assigned to adsorbed water. The spectra in Figures 8b and 8d were obtained after exposing the samples in (a) and (c) to 2 Torr of pyridine, followed by evacuation. In both cases, the only bands observed for pyridine are those associated with Lewis sites (1454 cm^{-1}). There was no evidence for the formation of pyridinium ions at 1541 cm^{-1} consistent with reports in the literature summarized by Morterra and Magnacca.[28]

CONCLUSIONS

The results in this study demonstrate that the γ-Al_2O_3 acts as a Lewis acid in its interactions with simple alcohols. The adsorption of water simply blocks the reactive sites but does not introduce Brønsted acidity. Reaction of adsorbed alcohols occurs through a TS that has carbenium-ion character, as demonstrated by both DFT calculations and measured activation energies for reaction of various adsorbed alcohols.

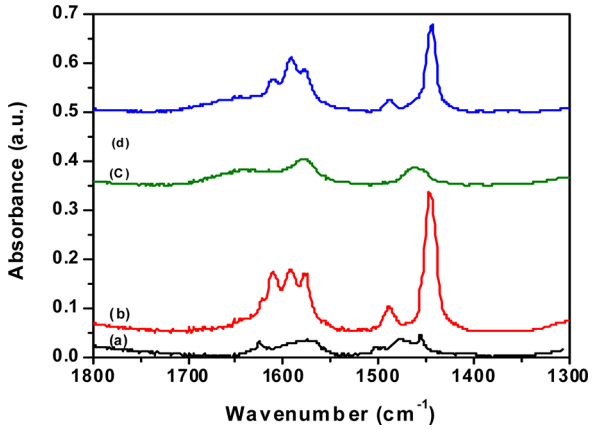

Figure 8. FTIR spectra recorded at 30 °C. All samples were treated in flowing dry air to 500 °C in flowing dry air prior to degassing under vacuum (4.0×10^{-2} Torr) for 1 h. (a) γ-Al_2O_3 (b) Pyridine (3 Torr) was dosed at 30 °C for 0.5 h, and the sample was subsequently degassed to 4.0×10^{-2} Torr to remove physisorbed pyridine. (c) The sample was exposed to water vapor (8.0 Torr) at 300 °C for 0.3 h. (d) Pyridine (2 Torr) was dosed to the sample in (c) at 30 °C for 0.5 h, the sample was subsequently degassed to 4.0×10^{-2} Torr to remove physisorbed pyridine.

Finally, alkali impurities significantly affect the reactivity of γ-Al_2O_3, making it very important that catalytic studies be carried out on pure forms of the material.

■ ASSOCIATED CONTENT

Supporting Information

Further details are given in Table 1S and Figures 1S–6S. This material is available free of charge via the Internet at http://pubs.acs.org.

■ AUTHOR INFORMATION

Corresponding Author

*Phone: +1 215 898 4439. Fax: +1 215 573 2093. E-mail: gorte@seas.upenn.edu.

Notes

The authors declare no competing financial interest.

■ ACKNOWLEDGMENTS

This work was supported as part of the Catalysis Center for Energy Innovation, an Energy Frontier Research Center funded by the U.S. Department of Energy, Office of Science, Office of Basic Energy Sciences under Award no. DE-SC0001004. The authors are thankful to Air Products and Chemicals, Inc for trace level sodium analyses.

■ REFERENCES

(1) Gorte, R. J. *Catal. Lett.* **1999**, *62*, 1–13.
(2) Makgoba, N. P.; Sakuneka, T. M.; Koortzen, J. G.; Schalkwyk, C.; Botha, J. M.; Nicolaides, C. P. *Appl. Catal., A* **2006**, *297*, 145–150.
(3) Reichle, W. T. *J. Catal.* **1980**, *63*, 295–306.
(4) Knözinger, H. *Angew. Chem., Int. Ed. Engl.* **1968**, *7*, 791–805.
(5) Knözinger, H.; Bühl, H.; Kochloefl, K. *J. Catal.* **1972**, *24*, 57–68.
(6) Knözinger, H.; Ratnasamy, P. *Catal. Rev.- Sci. Eng.* **1978**, *17*, 31–70.
(7) Morterra, C.; Ghiotti, G.; Boccuzzi, F.; Coluccia, S. *J. Catal.* **1978**, *51*, 299–313.
(8) Digne, M.; Sautet, P.; Raybaud, P.; Euzen, P.; Toulhoat, H. *J. Catal.* **2002**, *211*, 1–5.
(9) Clayborne, P. A.; Nelson, T. C.; DeVore, T. C. *Appl. Catal., A* **2004**, *257*, 225–233.
(10) Feng, G.; Huo, C. F.; Deng, C. M.; Huang, L.; Li, Y. W.; Wang, J.; Jiao, H. *J. Mol. Catal. A: Chem.* **2009**, *304*, 58–64.
(11) Kwak, J. H.; Mei, D.; Peden, C. H. F.; Rousseau, R.; Szanyi, J. *Catal. Lett.* **2011**, *141*, 649–655.
(12) Parrillo, D. J.; Gorte, R. J.; Farneth, W. E. *J. Am. Chem. Soc.* **1993**, *115*, 12441–12445.
(13) Shinohara, Y.; Nakajima., T.; Suzuki, S. *J. Mol. Struct.* **1999**, *460*, 231–244.
(14) Becke, A. D. *J. Chem. Phys.* **1993**, *98*, 5648–5652.
(15) Lee, C. T.; Yang, W. T.; Parr, R. G. *Phys. Rev. B* **1988**, *37*, 785–789.
(16) Frisch, M. J.; Trucks, G. W.; Schlegel, H. B.; Scuseria, G. E.; Robb, M. A.; Cheeseman, J. R.; Scalmani, G.; Barone, V.; Mennucci, B.; Petersson, G. A.; Nakatsuji, H.; Caricato, M.; Li, X.; Hratchian, H. P.; Izmaylov, A. F.; Bloino, J.; Zheng, G.; Sonnenberg, J. L.; Hada, M.; Ehara, M.; Toyota, K.; Fukuda, R.; Hasegawa, J.; Ishida, M.; Nakajima, T.; Honda, Y.; Kitao, O.; Nakai, H.; Vreven, T.; Montgomery, Jr., J. A.; Peralta, J. E.; Ogliaro, F.; Bearpark, M.; Heyd, J. J.; Brothers, E.; Kudin, K. N.; Staroverov, V. N.; Kobayashi, R.; Normand, J.; Raghavachari, K.; Rendell, A.; Burant, J. C.; Iyengar, S. S.; Tomasi, J.; Cossi, M.; Rega, N.; Millam, N. J.; Klene, M.; Knox, J. E.; Cross, J. B.; Bakken, V.; Adamo, C.; Jaramillo, J.; Gomperts, R.; Stratmann, R. E.; Yazyev, O.; Austin, A. J.; Cammi, R.; Pomelli, C.; Ochterski, J. W.; Martin, R. L.; Morokuma, K.; Zakrzewski, V. G.; Voth, G. A.; Salvador, P.; Dannenberg, J. J.; Dapprich, S.; Daniels, A. D.; Farkas, Ö.; Foresman, J. B.; Ortiz, J. V.; Cioslowski, J.; Fox, D. J. *Gaussian 09*, Revision A.1; Gaussian, Inc.: Wallingford, CT, 2009.
(17) Srinivasan, S.; Narayanan, C. R.; Biaglow, A.; Gorte, R.; Datye, A. K. *Appl. Catal., A* **1995**, *132*, 271–287.
(18) Redhead, P. A. *Vacuum* **1963**, *12*, 203–211.
(19) Demmin, R. A.; Gorte, R. J. *J. Catal.* **1984**, *90*, 32–39.
(20) Maresca, O.; Allouche, A.; Aycard, J. P.; Rajzmann, M.; Clemendot, S.; Hutschka, F. *J. Mol. Struct.* **2000**, *505*, 81–94 and references therein.
(21) Wittbrodt, J. M.; Hase, W. L.; Schlegel, H. B. *J. Phys. Chem. B* **1998**, *102*, 6539–6548.
(22) Wischert, R.; Copéret, C.; Delbecq, F.; Sautet, P. *Chem. Commun.* **2011**, *47*, 4890–4892.
(23) Joubert, J.; Delbecq, F.; Sautet, P. *J. Catal.* **2007**, *251*, 507–513.
(24) Kwak, J. H.; Rousseau, R. J.; Mei, D.; Peden, C. H. F.; Szanyi, J. *ChemCatChem.* **2011**, *3*, 1557–1561.
(25) Joubert, J.; Delbecq, F.; Sautet, P. *J. Catal.* **2007**, *251*, 507–513.
(26) Dabbagh, H. A.; Zamani, M.; Davis, B. H. *J. Mol. Catal. A: Chem.* **2010**, *333*, 54–68.
(27) Hendriksen, B. A.; Pearce, D. R.; Rudham, R. *J. Catal.* **1972**, *24*, 82–87.
(28) Morterra, C.; Magnacca, G. *Catal. Today* **1996**, *27*, 497–532.
(29) Blanksby, S. J.; Ellison, B. G. *Acc. Chem. Res.* **2003**, *36*, 255–263.